Journal of Engineering Science and Technology
Vol. 15, No. 1 (2020) 001 - 021

HYBRID H-INFINITY FUZZY LOGIC CONTROLLER DESIGN

MOHAMMED Y. HASSAN, HAZEM I. ALI, HAIDER M. JASSIM*

Control and Systems Engineering Department, University of Technology - Iraq
*Corresponding Author: 60168@uotechnology.edu.iq

Abstract

Since there is a lot of parallelism between H-infinity and the interval type-2 fuzzy logic control and they may complement one another, a new hybrid controller is proposed which combines their capabilities. This controller is proposed to assure both robust stability and robust performance of uncertain and nonlinear systems. It is shown that this controller is more efficient in achieving better performance for coupled-nonlinear systems than if only one of them is used. Furthermore, it demonstrates high robustness capabilities in the presence of large uncertainties in the system parameters. The effectiveness of the proposed controller is verified using highly nonlinear, MIMO and uncertain human swing lag system under different test scenarios. The tests reveal that the proposed controller has significantly improved the system performance as compared with the implementation of the classical H-infinity controller. The tracking performance has been enhanced by (94.7%), while the disturbance rejection performance has been refined by (13.8%). However, the most considerable improvement has been recorded for the robustness to system parameters changes with (98%).

Keywords: Coupled-nonlinear systems, H-infinity, Human swing leg system, IT2-FLC, Robust control.

1. Introduction

Nonlinear-coupled multivariable systems are increasingly posing a significant challenge to the control community. Complicated and usually multi-loop controllers are being employed to overcome the influence of the nonlinear interaction between input and output variables. For most of these control algorithms, the system performance is compromised with the robust stability to tackle the uncertainties produced by modelling errors and external disturbances [1]. A controller is required to decouple and isolate the controlled variables such that a change in one variable will result in a minimal effect on other system variables. Furthermore, it is desirable that the proposed controller will have the capacity to deal with a wide spectrum of uncertainties and disturbances while maintaining the output performance of the system.

Fuzzy logic controllers (FLCs) have inspired a lot of research in this field with recorded success in dealing with poorly modelled dynamics. The significant implications of the uncertainties and disturbances cannot be dealt with using the crisp membership functions of the conventional fuzzy logic, which results in degradation in the efficiency [1]. For this reason, Zadeh introduced the concept of Interval Type-2 Fuzzy Logic (IT2 FL) which is considered a generalization and extension of the type-1 fuzzy logic [2]. The new algorithm has added an extra degree of freedom to the fuzzy logic system, which enables it to efficiently model and handle higher levels of uncertainties [3].

Unlike the conventional fuzzy logic, the IT2 FL produces an interval representation for each crisp value in the input universe of discourse, while the membership function is characterized by upper and lower bounds. Then an order reduction method is implemented on the IT2 FL output to convert it to a type-1 FL output by utilizing the Karnik–Mendel (KM) algorithm, which is the commonly adopted type-reduction method [4]. This resulted in a powerful tool, which outperformed the conventional type fuzzy logic controllers. It offered a better tracking and disturbance rejection performance when applied to a linear quadruple-tank system, which has significant interactions between its variables [5].

Barkat et al. presented another successful application of the IT2 FL in tackling interactions between the speed and the electric current of permanent magnet synchronous motor [6]. The decoupling was accomplished by introducing a sliding surface term and adapting the IT2 FL systems to cope with the unavoidable reconstructions between the subsystems. However, the simulation of the phase current demonstrated high chattering effect due to the sliding mode switching effect. An interval type-2 fractional-order fuzzy logic controller was proposed as trajectory tracking algorithm for redundant robot manipulator [1]. It has been shown that the interval type-2 FL required less rules than the type-1 FL to perform the same task. Nevertheless, an optimization algorithm was invoked to tune the fractional-order controller gains and the derivative order to obtain the desired performance.

Another application of the IT2 FL system in the field of coupled multivariable system has been presented by Zeghlache et al. [7]. The control strategy was based on the sliding mode control technique while the IT2 has been used to minimize the uncertainties produced by residual of the feedback linearization component of the controller. Biglarbegian et al. [8[proposed a novel inference mechanism based on the Takagi-Sugeno-Kang (TSK) model, which enables a more feasible stability analysis method. Moreover, El-Nagar and El-Bardini [9] claimed that the IT2 FL controllers

that employs Wu-Mendel algorithm for type reduction are more suitable for real-time application since it establishes uncertainty bounds to approximate the type reduction operation.

On the other hand, H-infinity control has been used to both stabilize and decouple nonlinear multivariable systems, which can be linearized around nominal values. The H-infinity optimal control theory is based on synthesizing a controller that minimizes the infinite norm of the closed-loop control by restricting the sizes of both signals and transfer functions [10].

The controller was applied to track a desired trajectory of MIMO twin rotor system while coping with a certain level of parameters uncertainty which is mainly due obtaining the model through an identification process [11]. Rigatos et al. proposed an H-infinity controller to control the angular speed and the magnetic flux of asynchronous train motors [12].

Bagherieh, and Horowitz [13] combined the design objectives of the H2 and the H-infinity controllers depending on the frequency response of the gathered data. The H-infinity component was used to shape the closed loop transfer function and guarantee closed loop stability while H2 norm was employed to constrain the time domain signals and enhance the transient response. Unlike other nonlinear robust controllers, the H-infinity design requires rough knowledge about the magnitudes of the uncertainties and disturbances [14].

For this reason, H-infinity controller is usually fused with other nonlinear controllers to grasp the merits of both designs and minimize their disadvantages. For instance, an adaptive fuzzy H-infinity controller was proposed to track the attitude of a specific trajectory during a reusable launching vehicle re-entry phase [15]. Another example is the combination between IT2 FLC and the H-infinity controller, which was used to control a special class of nonlinear singular systems with time-delay [16].

Stabilization was assured by a multi-loop H-infinity controller while the IT2 FL was introduced to model the uncertain nonlinear system. Meziane and Boumhidi proposed a multi-machine controller that incorporates both interval type-2 FL and the optimal H-infinity controllers [17]. The IT2 task was to stabilize the power system while the optimal tracking performance was accomplished by the H-infinity controller. However, the integration method, by simply adding the two terms, will have the jeopardy of introducing large peaks in the input signals, due to the fact that both controllers will attempt to compensate for the error at the same instant, which will be accumulated as the actuation signal and result in large input peaks.

The Problem that this research is aiming to solve is to design an input that controls the following general nonlinear multivariable system

$$\dot{x} = f(t, x(t), u(t)) \tag{1}$$

where $f(.)$ is a nonlinear function of time t, states $x(.)$, and input $u(.)$ variables, whereas the state and the input vectors $x, u \in R^{n\times 1}$. It is assumed that the system has a complex nonlinear relation between its variables, which involve interactions between input channels. It is also assumed that the system is inherently unstable with external disturbances affecting its state variables. To make it more challenging, the system parameters are considered to be uncertain or changing. This paper differs from other researches in this field by proposing a controller that handles a significant change in the model parameters while maintaining the tracking performance and

disturbance rejection properties. The rest of this paper will be organized as follows: Section 2 introduces and establish the theoretical bases of our proposed controller. The proposed controller is applied to an illustrative example and a comparison between its results and the results obtained from the ordinary H-infinity controller is given in Section 3. Then conclusion is presented in Section 4.

2. Controller Design

It is desirable to synthesize a controller that can stabilize the system shown in Eq. (1) and decouple the input variables by extracting $u(t)$ term out of the function brackets. This can be achieved by employing a state feedback H-infinity controller, which requires conducting a linearization process on the nonlinear system around certain operating point. Although it is based on the linear model, the design can cope with uncertainties produced by drifting away from where the system is linearized. However, this implies that in order to maintain stability in wider region around the operating point, the controller trades-off the closed loop performance by the robust stability. An interval type-2 fuzzy logic controller (IT2 PI-FLC) will be utilized to enhance the performance of the system by injecting extra control input and minimizes the tracking error. Furthermore, the IT2 PI-FLC is separately designed and merged with the H-infinity controller because of the proposed integration method that resembles a cascade structure. The IT2 PI-FLC takes the advantage of H-infinity decoupling feature to simplify its design and tuning. Thus, a simple manual tuning could be implemented instead of complicated optimization techniques required to tune such controllers.

2.1. H-infinity control

The optimal H-infinity controller is implemented to reduce the effect of the worst-case uncertainties, external disturbances, and nominal inputs on the closed-loop performance of a linearized plant. The H-infinity algorithm is essentially a model-based technique, which shapes a feedback controller that minimizes the maximum peak in the magnitude response of a particular uncertain system. To solve the problem in a unified framework, the nonlinear multivariable system described by Eq. (1) is linearized and rewritten as a generalized state-space equation [10]

$$P := \begin{cases} \dot{x} = Ax + B_1 w + B_2 u \\ z = C_1 x + D_{11} w + D_{12} u \\ y = C_2 x + D_{21} w + D_{22} u \end{cases} \tag{2}$$

where z and y are the error output and measured output respectively, while w represents the disturbance input which encompasses parameter perturbation, noises, and environmental disturbances signals. Figure 1 shows the general H-infinity control structure where K represents the state feedback controller. The objective of this controller is to minimize the infinite norm of the singular values of the generalized plant frequency response

$$\|P\|_\infty \triangleq \max_{w \in \mathbb{R}} |p(jw)| \tag{3}$$

$$\|P\|_\infty < \gamma_\infty \tag{4}$$

where γ_∞ represents a constant upper bound on disturbances and uncertainties that can be treated by the control signal. Equation (3) can be reformed into a cost function J composed of the error output and the disturbance input signal. The disturbance input

w attempts to maximize the cost function, whereas the control input u functions to minimize it. The cost function can be expressed as [18, 19]

$$J(z,w) = \int_0^\infty z^T z + \gamma_\infty^2 w^T w \tag{5}$$

Now, let $\gamma_\infty > 0$ and $G(s) := (A, B, C, 0)$, where A, B, and C are the linearized system state-matrices. There exist a matrix $Q \geq 0$ such that [18]

$$QA + A^T Q + \gamma_\infty^{-2}\, Q\, BB^T Q + C^T C = 0 \tag{6}$$

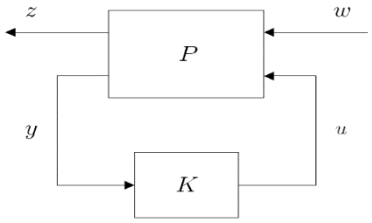

Fig. 1. Generalized H-infinity controller structure.

and the term $A + \gamma_\infty^{-2}\, BB^T Q$ has no eigenvalues on the imaginary axis, which results in $\|G\|_\infty < \gamma_\infty$.

Proof: assume that $Q \geq 0$, and let

$$W(s) := \begin{bmatrix} A & -B \\ B^T Q & \gamma_\infty^2 I \end{bmatrix} \tag{7}$$

$$W^{-1}(s) := \begin{bmatrix} A + \gamma_\infty^{-2} BB^T Q & \gamma_\infty^{-2} B \\ \gamma_\infty^{-2} B^T Q & \gamma_\infty^{-2} I \end{bmatrix} \tag{8}$$

Equation (7) has no zeros on the imaginary axis, since Eq. (8) has no poles on the imaginary axis. Then by substituting the matrix A in Eq. (6) by the term $-(j\omega I - A)$ yields

$$-Q(j\omega I - A) - (j\omega I - A)^* Q + \gamma_\infty^{-2} QBB^T Q + C^T C = 0 \tag{9}$$

By multiplying Eq. (9) by $B^T (j\omega I - A)^{*-1}$ on the left and $(j\omega I - A)^{-1} B$ on the right and completing the square, the following equation is obtained

$$G^*(j\omega) G(j\omega) - \gamma_\infty^2 I + \gamma_\infty^{-2} W^*(j\omega) W(j\omega) = 0 \tag{10}$$

This gives

$$G^*(j\omega) G(j\omega) = \gamma_\infty^2 I - \gamma_\infty^{-2} W^*(j\omega) W(j\omega) = 0 \tag{11}$$

Since $W(s)$ has no zeros on the imaginary axis, we establish that $\|G\|_\infty < \gamma_\infty$.

Theorem: if the generalized control system P satisfies the following conditions [10]:

- (A, B_2, C_2) Stabilizable and detectable.
- D_{12} and D_{21} have full rank.
- $\begin{bmatrix} A - j\omega I & B_2 \\ C_1 & D_{12} \end{bmatrix}$ has full column rank $\forall \omega$.

- $\begin{bmatrix} A - j\omega I & B_1 \\ C_2 & D_{21} \end{bmatrix}$ has full column rank $\forall \omega$.
- $D_{11} = 0$ and $D_{22} = 0$.

Then, there exist a solution for the following algebraic Riccati equation

$$QA + A^T Q + Q(\gamma_\infty^{-2} B_1 B_1^T - B_2 B_2^T)Q + C_1^T C_1 = 0 \quad (12)$$

Considering that

$$Re\,\{\lambda_i[A + (\gamma_\infty^{-2} B_1 B_1^T - B_2 B_2^T)Q]\} < 0, \ \forall i \quad (13)$$

Therefore, the robust controller K, which is capable of minimizing the influence of uncertainties and disturbances on the closed loop control system, can be formulated as

$$K = B_2^T Q \quad (14)$$

while the stabilizing control signal is

$$u(t) = -Kx(t) \quad (15)$$

2.2. Interval Type-2 FLC (IT2 FLC)

Interval type-2 fuzzy logic system has been proposed to handle the uncertainties imposed by the non-modelled dynamics and the external disturbances. The structure of IT2 FLC demonstrated in Fig. 2 is quite similar to its Interval type-1 fuzzy logic controller IT1 FLC counterpart. The major difference is the higher dimensional membership functions, which composed of an extra dimension to express the magnitude of the uncertainties. The footprint of uncertainty [16], which is the area bounded by the upper and the lower membership functions shown in Fig. 3, is a direct consequence of these uncertainties implications. The presence of higher-order fuzzy logic component in the fuzzification stage will require a type-reduction process in the defuzzification stage.

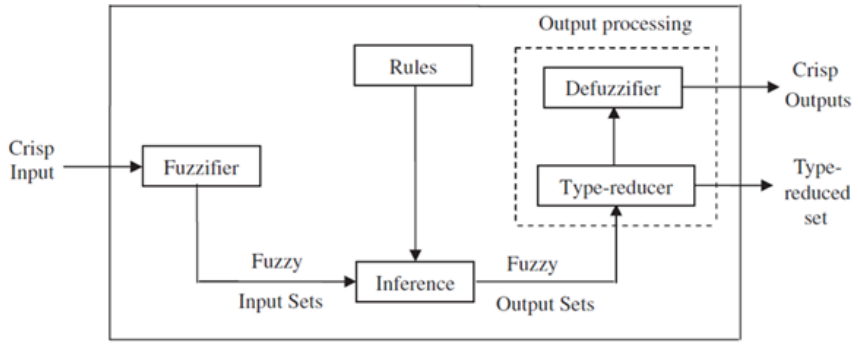

Fig. 2. IT2 FLC System structure [20].

The Fuzzifier maps a crisp n inputs values $x = [x_1, \ldots\ldots, x_n]$ into fuzzy set space. As can be seen in Fig. 3, the input value is projected on the membership functions, which resulted in an interval represented by the intersection with the upper and lower bounds. The Rule base block encompasses the principle knowledge base expressed in form of "If…then" statements. Considering that the

IT2 system contains N rules, the conditional statements will have the following general form

$$R^N\text{: } IF\ x_1\ is\ \tilde{F}_1^N\ and\ \ldots\ldots\ and\ x_i\ is\ \tilde{F}_i^N\ \ THEN\ y\ is\ Y^N \tag{16}$$

where $\tilde{F}_I^N$ $(I = 0 \ldots\ldots i)$ are terms that are modelled by the IT2 fuzzy sets, and Y^N is represented by the interval bounded by the lower and upper consequences $\left[\underline{y}^N, \overline{y}^N\right]$. The firing interval $\left[\underline{f}^N, \overline{f}^N\right]$ is to be calculated based on the input intersection with the upper MF $\overline{\mu}_{\tilde{F}_j^N}(x_j)$ and the lower MF $\underline{\mu}_{\tilde{F}_j^N}(x_j)$ combined with the antecedent rules. By utilizing the product expression of the i_{th} rule, the computation of the left and right firing points can be formulated as [21]

$$\underline{f}^N = \underline{\mu}_{\tilde{F}_1^N}(x_1) \times \underline{\mu}_{\tilde{F}_2^N}(x_2) \times \ldots\ldots \times \underline{\mu}_{\tilde{F}_n^N}(x_n) \tag{17}$$

$$\overline{f}^N = \overline{\mu}_{\tilde{F}_1^N}(x_1) \times \overline{\mu}_{\tilde{F}_2^N}(x_2) \times \ldots\ldots \times \overline{\mu}_{\tilde{F}_n^N}(x_n) \tag{18}$$

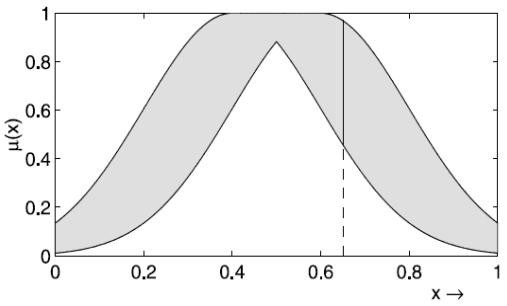

Fig. 3. An example of the upper and lower membership functions.

Subsequently, the type-2 fuzzy sets are reduced in order before performing the defuzzification process. This can be accomplished by using a type-reduction algorithm, which acts to combine the firing interval with the consequent of the corresponding rule. Although numerous methods have been developed to perform this task, the centre-of-sets type reduction method is the most commonly used method in the literature [6]. The final output can be expressed in the form of

$$y = [y_r, y_l] = \bigcup_{\substack{f^N \in F^N(x) \\ y^n \in Y^N}} \frac{\sum_{n=1}^{N} f^n y^n}{\sum_{n=1}^{N} f^n} \tag{19}$$

The two endpoints y_r and y_l can be found by

$$y_l = \frac{\sum_{n=1}^{L} \overline{f}^n \underline{y}^n + \sum_{n=L+1}^{N} \underline{f}^n \underline{y}^n}{\sum_{n=1}^{L} \overline{f}^n + \sum_{n=L+1}^{N} \underline{f}^n} \tag{20}$$

$$y_r = \frac{\sum_{n=1}^{R} \underline{f}^n \overline{y}^n + \sum_{n=R+1}^{N} \overline{f}^n \overline{y}^n}{\sum_{n=1}^{R} \underline{f}^n + \sum_{n=R+1}^{N} \overline{f}^n} \tag{21}$$

where $\overline{f}^n$ and $\underline{f}^n$ are the firing strength grades that correspond to the right and left most points, while R and N represent the switching points in which the accumulation functions change from the upper membership grades to the lower

membership grades and vice versa. An iterative KM algorithm is utilized to find these switching points for both right and left functions. In this research, the KM algorithm procedure for calculating the right and left points [21] has been followed. Although KM algorithm may require extensive and successive computations, it is still one of the most efficient and most adopted type-reduction method [8]. The defuzzification can be achieved by taking the average value of y_l and y_r. Thus, the defuzzified crisp output value becomes

$$y_{def} = \frac{y_l + y_r}{2} \tag{22}$$

2.3. IT2 H-infinity Controller Design

The IT2 FLC is combined with the H-infinity controller to overcome performance issues originated by assuming large bounds on the uncertainty while designing the robust feedback controller. By utilizing the H-infinity controller in tracking problem, the control signal demonstrated in Eq. (15) will have the form of

$$u(t) = Ke(t) \tag{23}$$

where $e(t)$ represents the error between the output and the desired input signals. Increasing the uncertainty in the system will require stricter robust stability conditions, which can be achieved at the expense of the feedback performance. This will result in a weaker control signal incapable of regulating the error signal to zero. Integrating the error signal may solve this deficiency, though the integral action is associated with deteriorating the transient response. Alternatively, a proportional plus integral action, which is based on the IT2 FLC, will be used to obtain the desired tracking performance. This controller will act to boost the error signal before being treated by the H-infinity controller, which will result in a more powerful control signal. The proposed IT2 PI-FL controller addition will not only enhance the tracking performance of the closed-loop control system but will also expand the limits in which the controller can comprehend high uncertainties. This is due to the robust nature of the two augmented controllers. Figure 4 illustrates the basic design of the IT2 PI-FLC. As can be seen in the figure, the IT2 FLC system accepts the error and its rate of change as an input in a PD-like fashion. Then by integrating the IT2 crisp output, an IT2 PI-FL controller action can be achieved. The controller gains K_I, K_P and K_d are associated with the integral, proportional, and derivative terms respectively. They will be used to adapt the IT2 controller by manipulating input and output signals to achieve a specified performance.

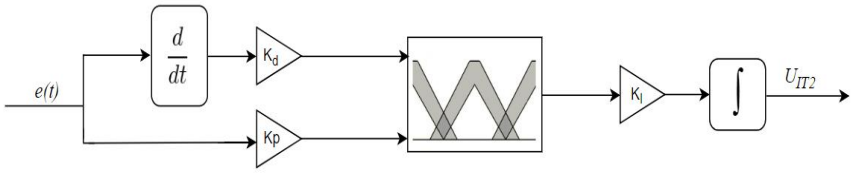

Fig. 4. IT2 PI- FLC.

The developed FL control signal will be applied to the H-infinity feedback controller, which will produce the following control signal

$$u(t) = K\, U_{IT2} \tag{24}$$

Because of the property of the H-infinity controller in decoupling the states of the system, the IT2 PI-FL controller will be uniquely employed on each error signal, which will significantly simplify its design. The block diagram of the complete control system can be seen in Fig. 5. Since the main objective of this controller is to be implemented on MIMO systems, it is assumed that all signals in the diagram are multi-dimensional. The notation n represents the number of output signals in the system, while m corresponds to the internal states that are not participating in the output signals of the system. These states are fed directly to the H-infinity controller to be regulated to their steady state values. Whereas the output signals are compared with the desired inputs to produce the error signals. Furthermore, the IT2 FLC block contains n IT2 PI-FL controllers that correspond to the number of those error signals.

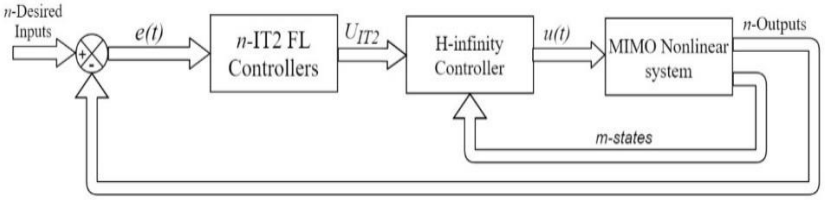

Fig. 5. IT2 PI-FL H-infinity Controller applied to MIMO nonlinear system.

3. Illustrative Example

In this section, the proposed controller will be validated by applying it to the Human Swing Leg (HSL) system. The human locomotion-gait activity is considered an inherently complicated task with highly nonlinear dynamics [22]. Building a humanoid robot with the capability of performing walking activity has various applications in the medical and military fields. The human swing leg is modelled as unconstrained double pendulum whose links are the thigh and shank of the human leg. The deflection angles of these two links will be provided by the hip and knee joints respectively, which connects the leg to the upper body. In an artificial human limb, the movement is provided by external motors torques, which considered as the manipulated input to the system model. A simplified schismatic representation of the unconstrained double pendulum is shown in Fig. 6. The hip and knee joints angles are represented by θ_1 and θ_2 respectively, while the two links are characterized by their length l and mass m.

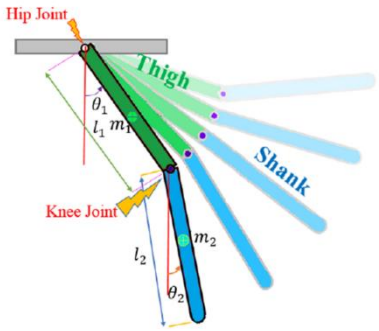

Fig. 6. Double pendulum representation of the HSL [23].

The mathematical model of the HSL system can be directly driven by finding the kinematic and potential energy of the unconstrained double pendulum and substituting them into the Euler-Lagrangian equation. The following state-space representation is obtained by adapting the associated models found in [22-24]

$$\dot{x}_1 = x_2 \tag{25}$$

$$\dot{x}_2 = x_4 \tag{26}$$

$$\dot{x}_3 = \frac{K_4(\tau_1 - K_2 x_4^2 \sin(x_1 - x_2) - K_3 \sin(x_1)) - K_2 \cos(x_1 - x_2)(\tau_2 + K_2 x_3^2 \sin(x_1 - x_2) - K_5 \sin(x_2))}{(K_1 K_4 - K_2^2 \cos(x_1 - x_2)^2)} \tag{27}$$

$$\dot{x}_4 = \frac{K_1(\tau_2 - K_2 x_3^2 \sin(x_1 - x_2) - K_5 \sin(x_2)) - K_2 \cos(x_1 - x_2)(\tau_1 + K_2 x_4^2 \sin(x_1 - x_2) - K_3 \sin(x_1))}{(K_1 K_4 - K_2^2 \cos(x_1 - x_2)^2)} \tag{28}$$

where the state variables are:

$x_1 = \theta_1$ (Angular position of thigh)

$x_2 = \theta_2$ (Angular position of shank)

$x_3 = \dot{\theta}_1$ (Angular velocity of thigh)

$x_4 = \dot{\theta}_2$ (Angular velocity of shank)

This model represents the mechanical relation between the two linked joints. As can be seen in the model, Eqs. (27) and (28) are highly nonlinear with extreme coupling between system variables. Other parameters found in the model are described as in Table 1.

Table 1. State-space model parameters [23].

Parameter	Description	Units
$\boldsymbol{\tau_1}$	Hip motor torque	N. m
$\boldsymbol{\tau_2}$	Knee motor torque	N. m
$\boldsymbol{g}$	Gravity force	$\mathrm{N/s^2}$
$\boldsymbol{K_1}$	$(m_1 + 4m_2)l_1^2/4$	$\mathrm{kg.\,m^2}$
$\boldsymbol{K_2}$	$m_2 l_1 l_2/2$	$\mathrm{kg.\,m^2}$
$\boldsymbol{K_3}$	$(m_1 + 2m_2)g l_1/2$	$\mathrm{kg.\,N.\,m/s^2}$
$\boldsymbol{K_4}$	$m_2\, l_2^2/4$	$\mathrm{kg.\,m^2}$
$\boldsymbol{K_5}$	$m_2\, g l_2/2$	$\mathrm{kg.\,N.\,m/s^2}$

The nonlinear model represented by Eqs. (25) to (28) can be linearized by performing the Jacobian method. The linearization process is carried out around the nominal values of states and inputs listed in Table 2.

Table 2. HSL nominal values and system parameters [23].

Parameter	Value
$\boldsymbol{\theta_1}$	30^o
$\boldsymbol{\theta_2}$	10^o
$\dot{\boldsymbol{\theta}}_{\boldsymbol{1}}$	22.92 deg/s
$\dot{\boldsymbol{\theta}}_{\boldsymbol{2}}$	17.19 deg/s
$\boldsymbol{\tau_1}$	0.5 N. m
$\boldsymbol{\tau_2}$	0.5 N. m
$\boldsymbol{m_1, m_2}$	0.1 kg
$\boldsymbol{l_1, l_2}$	0.55 m

The following linear state-space model has been obtained

$$\dot{x}(t) = Ax(t) + Bu(t) \tag{29}$$

$$y(t) = Cx(t) + Du(t) \tag{30}$$

where x is the states vector, y is the output of the system, while A, B, C and D are extracted from the Jacobian linearization process as

$$A = \begin{bmatrix} 0 & 1 & 0 & 0 \\ 0 & 0 & 0 & 1 \\ -18.9516 & 2.8818 & 0.2155 & -0.2174 \\ 20.2204 & -23.9036 & 0.6116 & 0.1796 \end{bmatrix},$$

$$B = \begin{bmatrix} 0 & 0 \\ 0 & 0 \\ 49.2616 & -69.4362 \\ -69.4362 & 197.0466 \end{bmatrix} \quad C = \begin{bmatrix} 1 & 0 & 0 & 0 \\ 0 & 1 & 0 & 0 \end{bmatrix} \quad D = \begin{bmatrix} 0 & 0 \\ 0 & 0 \end{bmatrix} \tag{31}$$

As illustrated in the previously, the HSL system has highly nonlinear dynamics with strong nonlinear coupling between variables. Since it is required to operate the system in different positions and with different desired input signals, it is nonviable to implement a simple linear controller, which is designed based on certain operating conditions. Thus, a more complicated control structure is needed to maintain an acceptable performance by the closed-loop system. However, before diving into such controller realization, an open-loop diagnosis must be conducted to fully comprehend the issues that required to be resolved by the proposed controller. Figure 7 shows the initial conditions response of the open-loop system. As seen in the figure, the unforced HSL system exhibits an unstable oscillatory response for both joints angles.

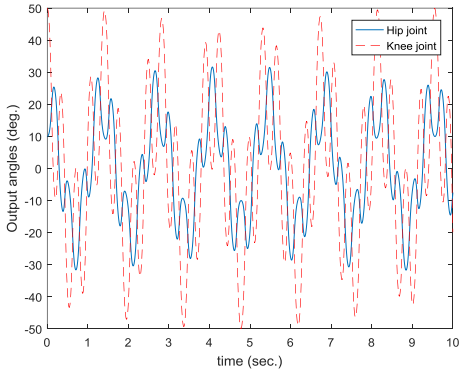

Fig. 7. HSL open-loop initial condition response.

3.1. H-infinity controller implementation

In this section, the H-infinity controller theory, which has been discussed in section 3, will be exploited. The controller gain matrix will be designed based on the linear state matrices shown in Eq. (31) and the H-infinity design procedure illustrated in Eqs. (12) to (14). The value of γ_∞ is chosen to be (1.23) which directly reflects the upper bound on uncertainties that can be tolerated by the H-infinity controller. Furthermore, it is assumed that input ($B_1 = B_2 = B$) which indicates that uncertainties and disturbances impact the system in the same direction as the input.

While the value of the observable output matrix C_1 is set to C. The value of H-infinity controller gain matrix is found by applying Eqs. (12) to (14) to be

$$K = \begin{bmatrix} 32.9699 & -0.4319 & 6.1050 & 0.2348 \\ -0.4211 & 29.1696 & 0.1993 & 5.5801 \end{bmatrix} \quad (32)$$

By feeding back the states of HSL system through this gain matrix and negating the sign of the resulted values as in Eq. (15), the robust control signals are computed. As a consequence, the states of the unforced system are stabilized and regulated to zero. Figure 8 shows the initial condition response of the closed-loop HSL system with the H-infinity controller. It is clear from the results that H-infinity controller acted rapidly to return the hip and knee joints angles and angular velocities to their steady-state values in less than (2 s). On the other hand, the controller exerted large torque values, which seems to be proportional to the initial starting angular position of the joint.

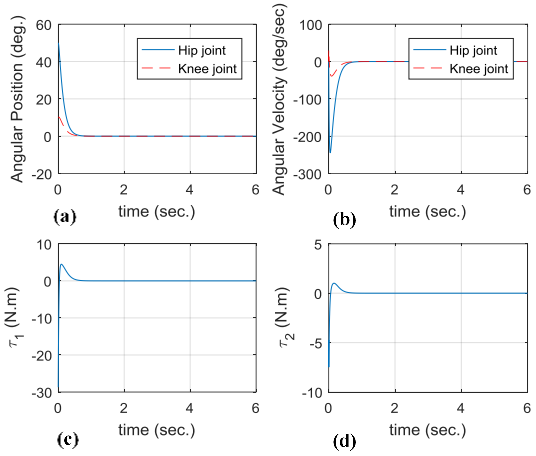

Fig. 8. HSL closed-loop initial condition response. (a- the angular position response for both joints, b- the angular velocity response for both joints, c- the torque input for the Hip joint, d- the torque input for the knee joint)

The controller in Eq. (15) can be modified to track a desired hip and knee angles by introducing the following error signal

$$e(t) = x_d(t) - x(t) \quad (33)$$

where x_d is the desired state-vector, which in this case written as

$$x_d = \begin{bmatrix} \theta^d_{hip}(t) \\ \theta^d_{Knee}(t) \\ 0 \\ 0 \end{bmatrix} \quad (34)$$

In order to compare the performance of the H-infinity controller with our proposed controller, a number of simulation scenarios will be examined. These scenarios are designed to reveal the effect of each controller on the performance of the closed-loop system. The scenarios will test tracking, disturbance rejection,

decoupling, and robustness capabilities of the H-infinity controller before and after the addition of IT2 PI-FL.

Scenario 1: testing the controller ability to track different desired input signals for both hip and knee joints. The controller should guarantee minimum interactions between the states of the system while minimizing the tracking error. The magnitudes of the desired inputs are chosen such that the system is driven outside the linearized region where the H-infinity controller has been designed. This will ensure to test the controllers ability to maintain steady performance in all regions

$$\theta_{hip}^{d}(t) = 50^{o} \times \sin(wt) \tag{35}$$

$$\theta_{Knee}^{d}(t) = 60^{o} \tag{36}$$

This scenario will be demonstrated in Figs. 9 and 13.

Scenario 2: applying a disturbance signal to the angular positions of the hip and knee joints. The disturbance may imply a sudden load change or the unconsidered effect of air-drag force. For this purpose, a typical step tracking problem will be employed with a pulse disturbance signal affecting both joints at a specific moment. This scenario will test the ability of the control algorithm to reject these disturbances by driving the states back to their steady-state location

$$\theta_{hip}^{d}(t) = 50^{o} \tag{37}$$

$$\theta_{Knee}^{d}(t) = 10^{o} \tag{38}$$

$$d_{\beta} = \beta \times [u(t-2) - u(t-3.5)] \tag{39}$$

where d_{β} is the disturbance signal being added directly to Eqs. (25) and (26), and β is the magnitude of that disturbance which is assumed here to be (10^{o}). The result of this scenario will be exhibited in Figs. 10 and 14.

Scenario 3: examines the robustness of the controller by determining the effect of changing the model parameters on the output performance of both joints. Step inputs of (60^{o}) and (50^{o}) will be applied on both hip and knee joints respective, while the response will be re-simulated for different parameter change percentage. A gradual change of (0%, 30%, 60%, and 80%) in the parameters will be introduced respectively. This effect can be observed in Figs.11 and 15.

Figure 9 shows scenario 1 results for the H-infinity controller. The tracking error in both joints is quite obvious, while the slight response distortion in the knee joint may be associated with the H-infinity failure to completely decoupling the system variables. On the other hand, the control signals maintain low values with a relatively large initial peak, which refer back to the previously discussed insufficiency of the H-infinity controller.

Scenario 2 simulation is demonstrated in Fig. 10. As can be seen in the figure, the closed-loop tracking performance exhibits steady-state errors, although the H-infinity controller has successfully rejected the effect of both rising and falling edges of the disturbance signal. While the input torque for the hip joint spikes to approximately (10 *N.m*) in an unavailing response to the large initial error. Considering the assumed HSL system parameters, this result indicates a larger and consequently heaver actuator must be used which might not be applicable.

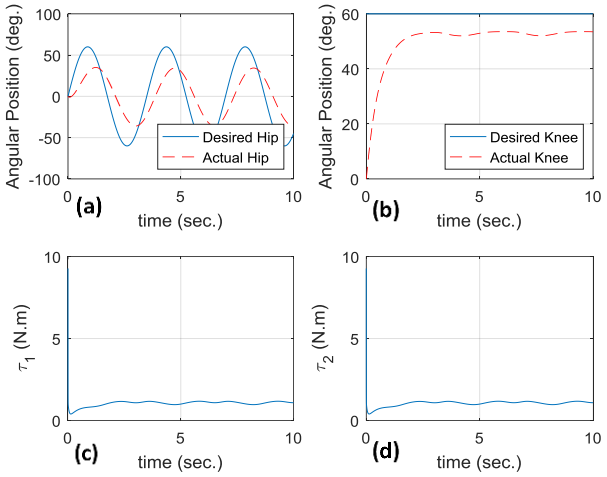

Fig. 9. H-infinity controller applied to scenario 1. (a- the desired and actual angular position of the hip joint, b- the desired and actual angular position of the knee joint, c- the torque input for the Hip joint, d- the torque input for the knee joint)

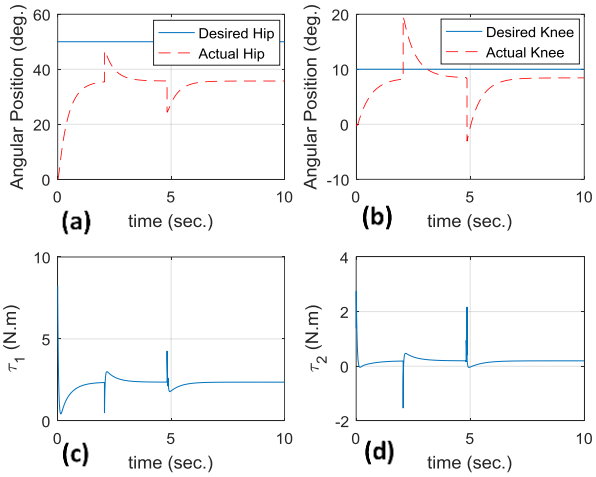

Fig. 10. H-infinity results for disturbance rejection scenario. (a- the desired and actual disturbed angular position of the Hip joint, b- the desired and actual disturbed angular position of the knee joint, c- the torque input for the Hip joint, d- the torque input for the knee joint).

It is expected that the H-infinity controller will have a satisfactory robust performance, because of the large uncertainty bounds, which have been initially assumed. According to what has been described in scenario 3, the parameters shown in Table 1 have been changed in values and the acquired results are plotted in Fig. 11. In the figure, changing the HSL system parameters did not alter the response dramatically. Instead, the figure shows that the error between the desired and actual angular positions is increased gradually as the uncertainties increased. This can be verified by examining the integral time absolute error (ITAE) performance index for each case, which is demonstrated in Table 4.

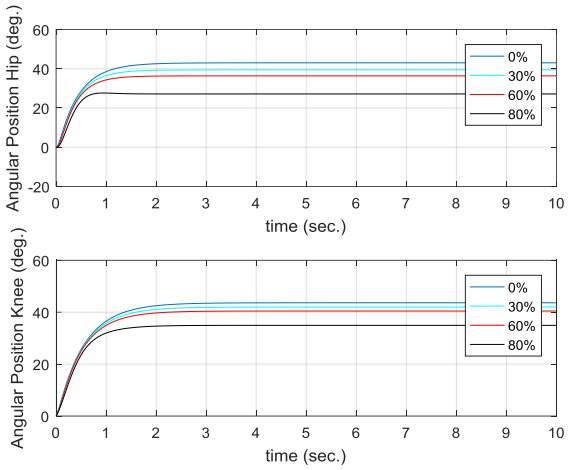

Fig. 11. H-infinity robust performance, Scenario 3.

3.2. Integral H-infinity controller

The integral action might be used to compensate for the error and enhance the steady-state performance of the system. The error signal is integrated before passing it through the H-infinity controller gain-matrix. Although this will immediately imply error elimination, the transient performance will deteriorate due to the uncontrolled compensation of the integral control action. Figure 12 shows the performance of such controller where a significant output oscillation has been recorded. The output stabilizes on the desired angles after approximately (40 s) while the input torques are a more applicable range as compared with the results obtained from the H-infinity controller. These results suggest that Integral H-infinity controller is not suitable for such application.

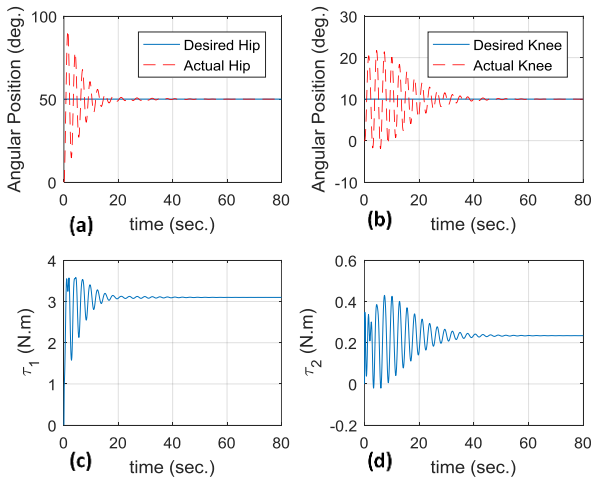

Fig. 12. Integral H-infinity controller performance. (a- the desired and actual angular position response of the Hip joint, b- the desired and actual angular position response of the knee joint, c- the torque input for the Hip joint, d- the torque input for the knee joint).

3.3. IT2 PI-FL H-infinity controller

This section investigates the performance of the IT2 H-infinity controller being implemented on the HSL system. The proposed controller design is explored in section 2.3 where the augmented controller structure ends-up containing different design parameters. These parameters, which include the IT2 PI-FLC gains and the H-infinity gain matrix, are to be tuned based on the desired performance of the controlled system.

For the HSL system, there are two outputs represented by the hip and knee joints angles, which indicates that it is required for two IT2 PI-FLC blocks to compensate for the error in each output. This will result in six parameters to tune to achieve the desired performance. Luckily, the H-infinity controller acts to decouple the system variables, which means that each IT2 PI-FLC block, can be tuned separately to obtain the desired response in the associated joint. Removing the stability and coupling issues out of the way can tremendously simplify the internal design of the IT2 FL system.

For this application, three triangular shaped membership functions are being implemented in the fuzzifier block shown in Fig. 2. Each membership function corresponds to a certain level of its input variable denoted by (High, Medium, and Low) levels. In general, there is no certain rule for selecting the shape of membership functions. However, for most control systems applications, the triangular shaped membership functions are popular because of their linear properties and relationships between their utilization and the reduction in steady-state error.

On the other hand, choosing the number of the input variables is a compromise between the accuracy of the result and the applicability of the controller. As the number of input variables increased, the accuracy of the IT2 FLC will be enhanced while the computation time will be rapidly increased which will result in a less applicable controller in a real-time context.

In this study, three-level input variables are employed because it is adequate for fast and reliable results. Since the IT2 FL system is being supplied with the error and its derivative, two identical fuzzifiers are used. While the rule-base system is designed based on the physical understanding of the error behaviour exhibited in Table 3, which in this case did not require any adaptation for the rules since the H-infinity controller facilitate design.

Table 3 represents a standard Rule-base model inspired by the usual behaviour of the error signal and its derivative and the intention to minimize their values. The defuzzification is executed using TSK model, which means that the output of the FL system is a crisp value with an associated level L demonstrated in the Rule-base table. During the adaptation of the output gain parameters of the IT2 FL controllers, the choice of using TSK model for defuzzification will prevent the exceedance of the output limits, which is a common problem in the mamdani-type defuzzifiers.

Table 3. IT2 FL system Rules.

$\dot{E}/E$	LOW	MEDIUM	HIGH
LOW	L_1	L_2	L_3
MEDIUM	L_2	L_3	L_4
HIGH	L_3	L_4	L_5

The H-infinity controller has the same structure and gains values shown in Eq. (32). On the other hand, since it is desirable to maintain a similar performance in

both joints, $K_I, K_P,$ and K_d gains in the two IT2 PI-FLC blocks are manually tuned, by using trial and error method, and selected as (8, 0.9 and 0.3) respectively in each. No soft computing method is required in this context since the tunning has been simplified by the hybrid nature of the controller structure, which successfully decoupled the two output variables.

Figure 13 demonstrates scenario 1 results of the proposed controller. In contrast to the results obtained from applying only the H-infinity controller, the tracking error has been significantly reduced and the fluctuations in the steady-state value of the knee joint have been minimized. In addition, the two control inputs do not experience the large initial peak as in the H-infinity scenario 1 simulations.

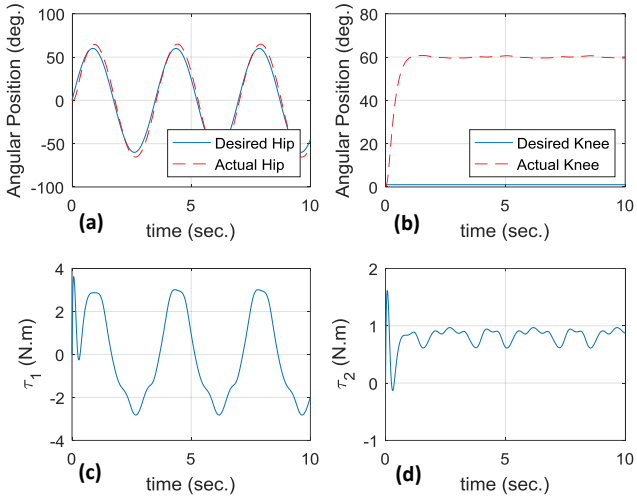

Fig. 13. IT2 PI-FL H-infinity controller results for scenario 1. (a- the desired and actual tracking response of the Hip joint, b- the desired and actual tracking response of the knee joint, c- the torque input for the Hip joint, d- the torque input for the knee joint).

Table 4 offers a holistic insight into the performance of each controller by examining the integral time absolute error (ITAE) performance index for each scenario. This index provides a better indication on not only the accumulated value of the error but also on how fast the controller reduces it over time. The table clearly shows the superiority of the proposed controller over the normal H-infinity control algorithm by demonstrating the value of the accumulated error of the two outputs angles over the simulation time. The table clearly shows that the IT2 PI-FL H-infinity controller produces significantly lower error values than the classical H-infinity controller for the simulated system. Moreover, it is worth mentioning that the IT2 H-infinity controller continued to maintain a steady performance even with a higher level of uncertainties and disturbances than the one shown in these simulations.

Figure 14 shows the performance of the proposed controller when subjected to a disturbance signal. The controller demonstrates disturbance rejection capabilities while maintaining a lower level of control inputs than the ones were required by the H-infinity controller in the same simulation scenario.

Table 4. ITAE measure of simulated scenarios for both controllers.

		H-INFINITY	IT2 H-INFINITY
SCENARIO 1		1.1668e+06	6.0848e+04
SCENARIO 2		5.6332e+04	4.8550e+04
SCENARIO 3	0 %	3.3744e+05	5.7971e+03
	30%	3.7364e+05	6.0038e+03
	60%	4.4757e+05	6.2195e+03
	80%	5.6436e+05	6.3660e+03

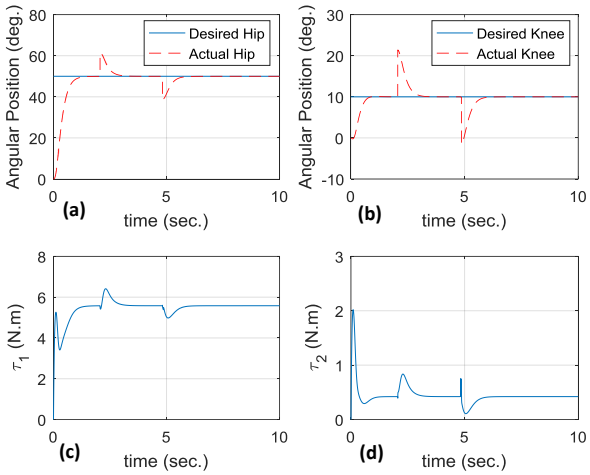

Fig. 14. IT2 PI-FL H-infinity results for disturbance rejection scenario. (a- the desired and actual disturbed angular position of the Hip joint, b- the desired and actual disturbed angular position of the knee joint, c- the torque input for the Hip joint, d- the torque input for the knee joint).

Finally, IT2 H-infinity controller outperforms the regular H-infinity in terms of robustness to system parameters variations. As can be seen in Fig. 15, changing the system parameters from (0% - 80%) has an inconsiderable effect on both the shape and steady state value of the output angles. This differs from the results obtained by implementing the H-infinity controller where the changes introduced observable changes in the output signals.

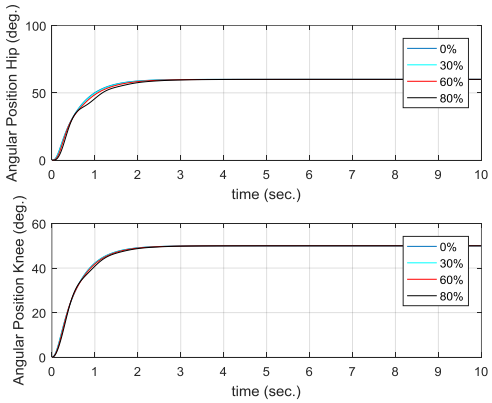

Fig. 15. IT2 PI-FL H-infinity controller robust performance, scenario 3.

4. Conclusion

A hybrid IT2 PI-FL H-infinity controller has been proposed in regards to a coupled-nonlinear MIMO system with uncertain parameters. The proposed control algorithm utilized the H-infinity capabilities in stabilizing and decoupling the complicated nonlinear system states, while the IT2 PI-FLC was added to enhance the system performance. The fusion between the two control algorithms has resulted in a powerful robust controller that can tolerate large uncertainties in the system parameters without compromising the system performance.

In order to show the validity of the proposed controller, it has been applied to a human swing lag system with a number of test scenarios designed specifically to reveal the controller properties. In comparison to the H-infinity only controller, the proposed controller demonstrated a superior performance for the same tasks. For simulation scenario 1, the output performance has been improved by (94.7%) from the H-infinity only case. This indicates that the IT2 PI-FL H-infinity is more efficient in tracking different desired input signals.

The improvement percentage has been calculated based on a ratio comparison between the steady-state values of the two output angles for both controllers taken the desired outputs in consideration. On the other hand, employing the IT2 PI-FL H-infinity controller in scenario 2 has resulted in less dramatic enhancement of (13.8%). This result establishes the fact that the choice of a large uncertainty bound in designing the H-infinity controller was sufficient to reject the bounded external disturbances. In this case, the IT2 PI-FL H-infinity controller addition merely eliminated the tracking error. Testing the robustness of the two controllers in scenario 3 has shown the exceptional capability of the IT2 H-infinity controller to maintain an average improvement of (98%). For this reason, it was conclusive that the proposed controller outperformed the normal H-infinity control algorithm.

Abbreviations

FLC	Fuzzy Logic Controller
HSL	Human Swing Leg
IT2 FLC	Interval Type 2 Fuzzy Logic Controller
ITAE	Integral Time Absolute Error
KM	Karnik–Mendel
TSK	Takagi-Sugeno-Kang

References

1. Kumar, A.; and Kumar, V. (2019). Design of interval type-2 fractional-order fuzzy logic controller for redundant robot with artificial bee colony. *Arabian Journal for Science and Engineering*, 44(3), 1883-1902.
2. Zadeh, L.A. (1975). The concept of a linguistic variable and its application to approximate reasoning. *Information sciences*, 8(3), 199-249.
3. Mendel, J.M.; John, R. I.; and Liu, F. (2006). Interval type-2 fuzzy logic systems made simple. *IEEE transactions on fuzzy systems*, 14(6), 808-821.
4. Karnik, N.N.; and Mendel, J.M. (2001). Centroid of a type-2 fuzzy set. *Information Sciences*, 132(1-4), 195-220.

5. Thangavelusamy, D.; Ponnusamy, L.; and Durairaj, S. (2017). Control of an ambiguous real time system using interval type 2 fuzzy logic control. *International Journal of Applied Engineering Research*, 12(21), 11383-11391.
6. Barkat, S.; Tlemçani, A.; and Nouri, H. (2011). Noninteracting adaptive control of PMSM using interval type-2 fuzzy logic systems. *IEEE Transactions on Fuzzy Systems*, 19(5), 925-936.
7. Zeghlache, S.; Kara, K.; and Saigaa, D. (2015). Fault tolerant control based on interval type-2 fuzzy sliding mode controller for coaxial trirotor aircraft. *ISA Transactions*, 59, 215-231.
8. Biglarbegian, M.; Melek, W.W.; and Mendel, J.M. (2010). On the stability of interval type-2 TSK fuzzy logic control systems. *IEEE Transactions on Systems, Man, and Cybernetics, Part B (Cybernetics)*, 40(3), 798-818.
9. El-Nagar, A.M.; and El-Bardini, M. (2014). Practical implementation for the interval type-2 fuzzy PID controller using a low cost microcontroller. *Ain Shams Engineering Journal*, 5(2), 475-487.
10. Alguefer, O.A. (2012). *Magnesium twin roll casting machine-modelling and control.* Doctoral Dissertation. McGill University, Montreal, Quebec, Canada.
11. Rao, V.S.; George, V.; Kamath, S.; and Shreesha, C. (2014). Reliable H infinity observer-controller design for sensor and actuator failure in TRMS. *Advances in Electrical Engineering (ICAEE), 2014 International Conference*. Vellore, India, 1-5.
12. Rigatos, G.; Siano, P.; Wira, P.; and Profumo, F.; (2015). Nonlinear H-infinity feedback control for asynchronous motors of electric trains. *Intelligent Industrial Systems*, 1(2), 85-98.
13. Bagherieh, O.; and Horowitz, R. (2018). Mixed H2/H-infinity data-driven control design for hard disk drives. Cornell University – systems and control, 1-23.
14. Koshy, R.; and Jayasree, P. (2017). Comparative study of H-infinity and sliding mode control for a manipulator with oscillatory-base. *Circuit, Power and Computing Technologies (ICCPCT), 2017 International Conference.* Kollam, India, 1-6.
15. Mao, Q.; Dou, L.; Zong, Q.; and Ding, Z. (2018). Attitude controller design for reusable launch vehicles during re-entry phase via compound adaptive fuzzy H-infinity control. *Aerospace Science and Technology*, 72, 36-48.
16. Tseng, C.L.; Wang, S.Y.; Liu, F.Y.; Jean, F.R.; and Fu, M.H. Robust type-2 TS fuzzy multiple feedback-loop H-infinity controller design for uncertain singular time-delay systems. (2016). *Systems, Man, and Cybernetics (SMC), 2016 IEEE International Conference*. Budapest, 3475-3480.
17. Meziane, K.B.; and Boumhidi, I. (2016). An interval type-2 fuzzy logic PSS with the optimal H∞ tracking control for multi-machine power system. *International Journal of Intelligent Engineering Informatics*, 4(3-4), 286-304.
18. Ali, H.I.; and Abdulridha, A.J. (2018). H-infinity based full state feedback controller design for human swing leg. *Engineering and Technology Journal*, 36(3A), 350-357.
19. Sinha, A. (2007). *Linear systems: optimal and robust control*. CRC press.

20. El-Bardini, M.; and M. El-Nagar, A. (2011). Direct adaptive interval type-2 fuzzy logic controller for the multivariable anaesthesia system. *Ain Shams Engineering Journal*, 2(3-4), 149-160.
21. Mendel, J.M. (2017). *Uncertain rule-based fuzzy systems: Introduction and New Directions* (2nd ed.). Springer International Publishing.
22. Eghtesad, Y.M.; Khoogar, A.; and Mohammad-Zadeh, A. (2015). Tracking control of a human swing leg as a double-pendulum considering self-impact joint constraint by feedback linearization method. *Journal of Control Engineering and Applied Informatics*, 17(1), 99-110.
23. Bazargan-Lari, Y.; Eghtesad, M.; Khoogar, A.R.; and Mohammad-Zadeh, A. (2015). Adaptive neural network control of a human swing leg as a double-pendulum considering self-impact joint constraint. *Transactions of the Canadian Society for Mechanical Engineering*, 39(2), 201-219
24. Bazargan-Lari, Y.; Gholipour, A.; Eghtesad, M.; Nouri, M.; and Sayadkooh, A. (2011). Dynamics and control of locomotion of one leg walking as self-impact double pendulum. *Control, Instrumentation and Automation (ICCIA), 2011 2nd International Conference*. Shiraz, Iran, 201-206.